# Epithelial Cytoskeletal Framework and Nuclear Matrix–Intermediate Filament Scaffold: Three-dimensional Organization and Protein Composition

EDWARD G. FEY, KATHERINE M. WAN, and SHELDON PENMAN
*Department of Biology, Massachusetts Institute of Technology, Cambridge, Massachusetts 02139*

ABSTRACT Madin-Darby canine kidney (MDCK) cells grow as differentiated, epithelial colonies that display tissue-like organization. We examined the structural elements underlying the colony morphology in situ using three consecutive extractions that produce well-defined fractions for both microscopy and biochemical analysis. First, soluble proteins and phospholipid were removed with Triton X-100 in a physiological buffer. The resulting skeletal framework retained nuclei, dense cytoplasmic filament networks, intercellular junctional complexes, and apical microvillar structures. Scanning electron microscopy showed that the apical cell morphology is largely unaltered by detergent extraction. Residual desmosomes, as can be seen in thin sections, were also well-preserved. The skeletal framework was visualized in three dimensions as an unembedded whole mount that revealed the filament networks that were masked in Epon-embedded thin sections of the same preparation. The topography of cytoskeletal filaments was relatively constant throughout the epithelial sheet, particularly across intercellular borders. This ordering of epithelial skeletal filaments across contiguous cell boundaries was in sharp contrast to the more independent organization of networks in autonomous cells such as fibroblasts. Further extraction removed the proteins of the salt-labile cytoskeleton and the chromatin as separate fractions, and left the nuclear matrix–intermediate filament (NM-IF) scaffold. The NM-IF contained only 5% of total cellular protein, but whole mount transmission electron microscopy and immunofluorescence showed that this scaffold was organized as in the intact epithelium. Immunoblots demonstrate that vimentin, cytokeratins, desmosomal proteins, and a 52,000-mol-wt nuclear matrix protein were found almost exclusively in the NM-IF scaffold. Vimentin was largely perinuclear while the cytokeratins were localized at the cell borders. The 52,000-mol-wt nuclear matrix protein was confined to the chromatin-depleted matrix and the desmosomal proteins were observed in punctate polygonal arrays at intercellular junctions. The filaments of the NM-IF were seen to be interconnected, via the desmosomes, over the entire epithelial colony. The differentiated epithelial morphology was reflected in both the cytoskeletal framework and the NM-IF scaffold.

A potentially powerful addition to the study of cell structure is afforded by combining detergent extraction with unembedded whole mount electron microscopy. In this protocol, soluble proteins are extracted with non-ionic detergent under near physiological conditions of ionic strength and pH. The cellular structure that remains after detergent extraction is called the skeletal framework (1, 2). The elaborate filament framework can be clearly seen using whole mount transmission electron microscopy, which omits conventional embedding, sectioning, and staining. We have observed the three-dimensional, anastomosing fiber networks in whole mounts of all cells we examined. These networks were largely masked in the conventional embedded sections of the same extracted material.

Previous reports using whole mount electron microscopy of detergent extracted cells have concentrated on the cytoskeletal organization of single cells, either fibroblasts or autonomous, malignant epithelial cells such as the HeLa line (2–10). In the study described here, we isolated and examined the interior architecture of cells organized as an epithelium.

THE JOURNAL OF CELL BIOLOGY · VOLUME 98 JUNE 1984 1973–1984

The architecture of cytoskeletal elements in these epithelial cells was profoundly different from that observed in single, autonomous cells. An ordering of structural elements appeared to contribute to the maintenance and possibly the genesis of differentiated tissue morphology. The experiments reported here used colonies of the well-characterized Madin-Darby canine kidney (MDCK)[1] cell line as a model epithelial tissue. Unlike most established cell lines of epithelial origin, the MDCK line has retained a highly differentiated phenotype and forms polarized colonies reminiscent of the distal kidney tubule epithelium (11) from which these cells were derived.

The structural elements of the MDCK epithelium were examined for protein composition and three-dimensional skeletal morphology using two previously described procedures (1–10). The skeletal framework was obtained by extraction of the soluble proteins with 0.5% Triton X-100 in a physiological buffer. It retained many of the morphological characteristics of the intact cells, but permits visualizing the topography of the internal fiber network with great clarity. The framework proteins were then removed as a salt-labile cytoskeleton fraction. Proteins associated with chromatin were removed by nuclease digestion and salt elution, leaving the nuclear matrix, intermediate filaments, and residual desmosomes as a highly organized array. This salt-resistant structure, for which we suggest the term nuclear matrix–intermediate filament (NM-IF) scaffold, affords striking three-dimensional views in whole mount transmission electron microscopy. The NM-IF scaffold contained virtually all of the cytokeratins, vimentin, desmosomal core proteins, and all of a protein marker for the nuclear matrix. Three-dimensional microscopy of the NM-IF scaffold shows that previously observed organization of cytokeratins and desmosomes (14–20) and of intermediate filaments with isolated nuclei (21–22) and nuclear matrices (10) are components of a global organization of these elements in epithelia. Intermediate filament networks branch out from the nuclear matrices and interconnect, via the desmosomes, throughout the entire epithelial tissue.

## MATERIALS AND METHODS

*Cell Culture:* MDCK cells were obtained from the laboratory of David Sabatini (New York University School of Medicine). Cells were used at a subconfluent density of $6–10 \times 10^6$ cells/100-mm diameter plastic tissue culture plate. Monolayer cultures of these cells were grown at 37°C in Dulbecco's medium supplemented with 10% fetal bovine serum (Gibco Laboratories, Grand Island, New York) in a humidified atmosphere of 5% $CO_2$.

*Cell Fractionation:* Plates of MDCK colonies were rinsed twice with phosphate-buffered saline (PBS), then extracted in cytoskeleton buffer (100 mM NaCl, 300 mM sucrose, 10 mM PIPES [pH 6.8], 3 mM $MgCl_2$, 0.5% Triton X-100 and 1.2 mM phenylmethylsulfonyl fluoride [CSK]) for 10 min at 0°C. The resulting "soluble" fraction was removed. An extraction buffer (250 mM ammonium sulfate, 300 mM sucrose, 10 mM PIPES [pH 6.8], 3 mM $MgCl_2$, 1.2 mM phenylmethylsulfonyl fluoride, and 0.5% Triton X-100) was added to the Triton X-100–insoluble structures for 10 min at 0°C and the "cytoskeleton" fraction was removed.

The "chromatin" fraction was removed from the remaining structural elements by digestion in a buffer identical to the CSK buffer except that 50 mM NaCl was present. To this buffer was added 100 μg/ml bovine pancreatic DNase/(EC 3.1.4.5, Worthington Biochemical Corp., Freehold, NJ), and 100 μg/ml pancreatic RNase A (EC 3.1.4.22, Sigma Chemical Co., St. Louis, MO) and digestion proceeded for 20 min at 20°C. Ammonium sulfate was added to a final concentration of 0.25 M and incubation continued for 5 min at 20°C. The "chromatin" fraction was removed as a supernatant (either directly from the monolayer or after a 10-min centrifugation at 10,000 $g_{avg}$) leaving the NM-IF fraction.

*Electron Microscopy:* For scanning electron microscopy, cells were grown on glass coverslips and fractionated as above. Cells were fixed at various stages of fractionation in the appropriate buffer containing 2.5% gluteraldehyde at 0°C for 30 min, followed by rinsing in 0.1 M sodium cacodylate and then 1% $OsO_4$ in 0.1 M Na cacodylate for 5 min at 0°C. The cells, still on coverslips, were dehydrated through an ethanol series, dried through the $CO_2$ critical point and sputter-coated with gold-palladium. The whole mount samples were examined in the lower stage of an ISI 2000 scanning electron microscope. Transmission electron miroscopy was done on cells grown on gold grids which were previously covered with formvar and coated with carbon. The cells were again fixed in 2.5% gluteraldehyde and processed as above. Grids of whole mount samples were examined in a JEM 100B transmission electron microscope. Thin sections were prepared from fractionated and fixed cell monolayers that were embedded in Epon-Araldite before sectioning. Sections were stained with lead citrate and uranyl acetate before examination in the JEM 100B as above. Immunolocalization of desmosomal proteins was carried out on formaldehyde-fixed NM-IF cores. Desmosomal antiserum (1:40) (kindly provided by M. Steinberg [Princeton University]) was added in cytoskeletal buffer containing 1% bovine serum albumin and incubated 30 min at 37°C. The grids were washed five times for a total of 25 min in CSK and 1% bovine serum albumin and incubated for an additional 30 min at 37°C in affinity-purified goat anti-rabbit IgG linked to 5-nm gold beads (Janssen Pharmaceutical, Beerse, Belgium). After extensive washing, these grids were postfixed and processed as described above.

*Monoclonal Antibody Production:* The hybridoma cell line producing monoclonal antibodies to a 52,000-mol-wt protein in the nuclear matrix was produced using established immunization and fusion protocols (23). This antibody resulted from a larger program of monoclonal antibody production to cytoskeletal and nuclear matrix proteins carried on in this laboratory by Drs. K. M. Wan and D. G. Capco. Details of the protocols used will be presented in a future publication (manuscript in preparation).

*Immunofluorescence Microscopy:* Immunofluorescence microscopy was performed using cells grown on glass coverslips. Whole cells were fixed and permeabilized in cold methanol for 10 min and fixed in 3.7% formaldehyde for 30 min at 0°C. NM-IF fractions were prepared from these cells as described above, and fixed in 3.7% formaldehyde for 30 minutes at 0°C. Fixed NM-IF scaffolds were extensively washed in PBS. Antibodies were applied at 1:100 dilution in PBS and coverslips were incubated 30 min at 37°C. Antibodies to keratins, desmosomal proteins and vimentin were generously provided by Drs. J. Rheinwald (Dana Farber Cancer Institute, Harvard Medical School), M. Steinberg (Princeton University), and R. Hynes (Center for Cancer Research, Massachusetts Institute of Technology), respectively. After extensive washing in PBS, the NM-IF fractions were incubated with goat anti-rabbit (or anti-mouse) IgG labeled with tetramethyl-rhodamine isothiocyanate (Sigma Chemical Co., St. Louis, MO) at a dilution of 1:40 for 30 min at 37°C. The labeled fractions were washed in PBS, mounted, and photographed using epifluorescence.

*Immunoblot Electrophoreses:* One-dimensional polyacrylamide gels were run according to the procedure described by Laemmli (24). Equal protein concentrations were loaded in comparing individual fractions. The reaction of antibodies to protein bands was visualized by the immunoblot technique on nitrocellulose paper (25). Nitrocellulose strips were incubated for 12 h in 2% hemoglobin in PBS, rinsed three times in PBS, and incubated for 2 h at 20°C with the relevant antibody diluted 1:40 in PBS. Excess antibody was washed with PBS (four washes, 20 min each). The strips were then incubated with goat anti-rabbit (or anti-mouse) IgG conjugated to horseradish peroxidase (1:300 dilution, Cappel Laboratories, Cochranville, PA) washed four times in PBS for a total of 80 min, then developed in 0.4 mg/ml 4-chloro-1-napthol in 0.01% (vol/vol) $H_2O_2$ (26).

The two-dimensional gel analysis was carried out according to the protocol of O'Farrell (27), except that the pH gradient used 0.4% (pH 5–7) and 1.6% (pH 3–10) ampholytes. Equivalent $^{35}S$ counts per minute were loaded to facilitate qualitative comparison.

## RESULTS

### Epithelial Skeletal Framework

The MDCK cell line is karyotypically stable, forms simple, cuboidal epithelial sheets in culture and retains many morphological and physiological characteristics of the distal tubule epithelium (11–13). The epithelial tissue sheets of MDCK

[1] *Abbreviations used in this paper:* CSK, 100 mM NaCl, 300 mM sucrose, 10 mM PIPES (pH 6.8), 3 mM $MgCl_2$, 0.5% Triton X-100, and 1.2 mM phenylmethylsulfonyl fluoride; MDCK, Madin-Darby canine kidney; NM-IF, nuclear matrix–intermediate filament; PBS, phosphate-buffered saline.

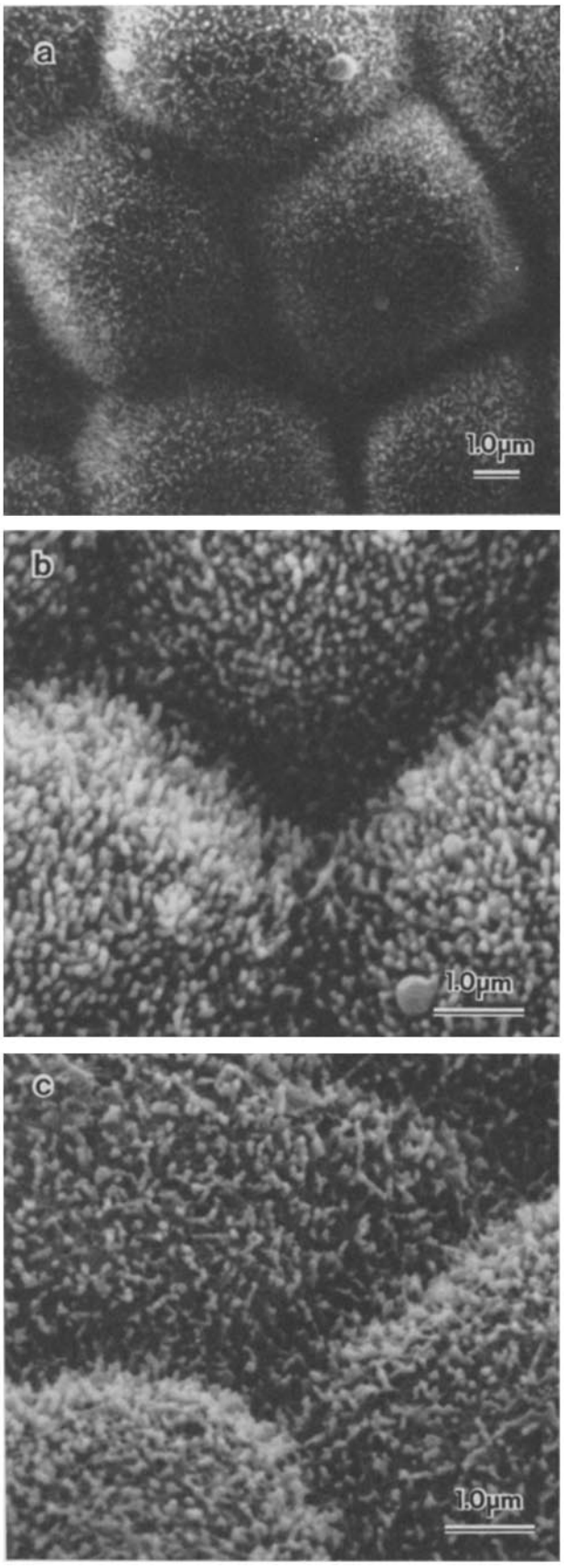


FIGURE 1 Scanning electron micrographs of MDCK apical surface morphology. Intact MDCK colonies were fixed, dehydrated, and dried through the $CO_2$ critical point and sputter coated with gold-palladium as described in Materials and Methods. They are seen in low magnification (*a*). The apical morphology is examined at high magnification in whole cells (*b*) and skeletal frameworks fixed after extraction in 0.5% Triton X-100 (*c*). (*a*) × 6,000. (*b*) × 13,000.

colonies grow as contiguous cells that possess an elaborate structural organization in which intercellular contact is maintained by tight junctions (zonula occludens), band junctions (zonula adherens), and desmosomes (maculae adherens) (14, 28). The cells are highly polarized and the apical surface of the MDCK colony is morphologically and biochemically distinct from the basolateral surface (28–32). For these reasons, the MDCK line serves as an excellent model of differentiated epithelial tissue.

The characteristic morphology of the MDCK colonies is shown in scanning electron micrographs (Fig. 1, *a* and *b*). The dome-shaped polygonal cells are densely covered with microvilli. The cell borders appear here as furrows between individual cells. The similarity of the morphology of these cultured cells to that of actual distal tubule epithelia is striking (33).

Fig. 1*c* shows the morphology, in scanning electron microscopy, of an MDCK colony after extraction with Triton X-100 in CSK buffer. Despite the removal of the soluble proteins (65% of the total) and most lipids (1, 34), the overall hemispheric configurations of both the cellular surfaces and borders are remarkably unchanged. The lipid-depleted microvilli are collapsed somewhat, but are present in the same density and have the distribution observed in the apical surface of intact MDCK colonies (Fig. 1*b*). These structures are similar to the intestinal brush border microvilli observed after extraction with Triton X-100 (35). The remnant microvilli are seen to project from a dense filamentous web (Fig. 1*c*). The extracted cell protein surface, visualized after the removal of lipids by the detergent, retains the morphology of the apical plasma membranes of intact cells. The maintenance of surface morphology by extracted structures has been observed in HeLa, 3T3, and CHO cell lines, and in chick myotubes (5, 36), and is probably due to the dense, anastomosing skeletal framework or fibers that appear to support the lipid-depleted surface.

## *Junctional Complexes in the Skeletal Framework*

Conventional Epon-embedded thin sections prepared from intact and Triton X-100 extracted cells are compared in Fig. 2. The intact cells (Fig. 2*a*) have the typical lightly staining interior seen by this method, while the extracted cells (Fig. 2, *b–d*) are largely empty save for many short filaments and polyribosomes that seem random in their distribution. Sections, cut perpendicular to the plane of the cell substrate (Fig. 2, *b* and *c*), show that the detergent extracted intercellular junctions have approximately the same localization and ultrastructure as their unextracted counterparts, suggesting that little or no distortion of the skeletal framework has occurred. The fine structure of the residual desmosomes (Fig. 2*d*) is readily identifiable after the removal of phospholipid and soluble protein. By these criteria, most of the desmosome core structure remains well-preserved in the skeletal framework (see below). The cytokeratins or tonofilaments (17) are partially visible as they pass through the plane of the section and they appear to be associated with the desmosomes. The residual junctional complexes, important to the establishment and maintenance of epithelial organization, appear to be well-preserved in the extracted cells.

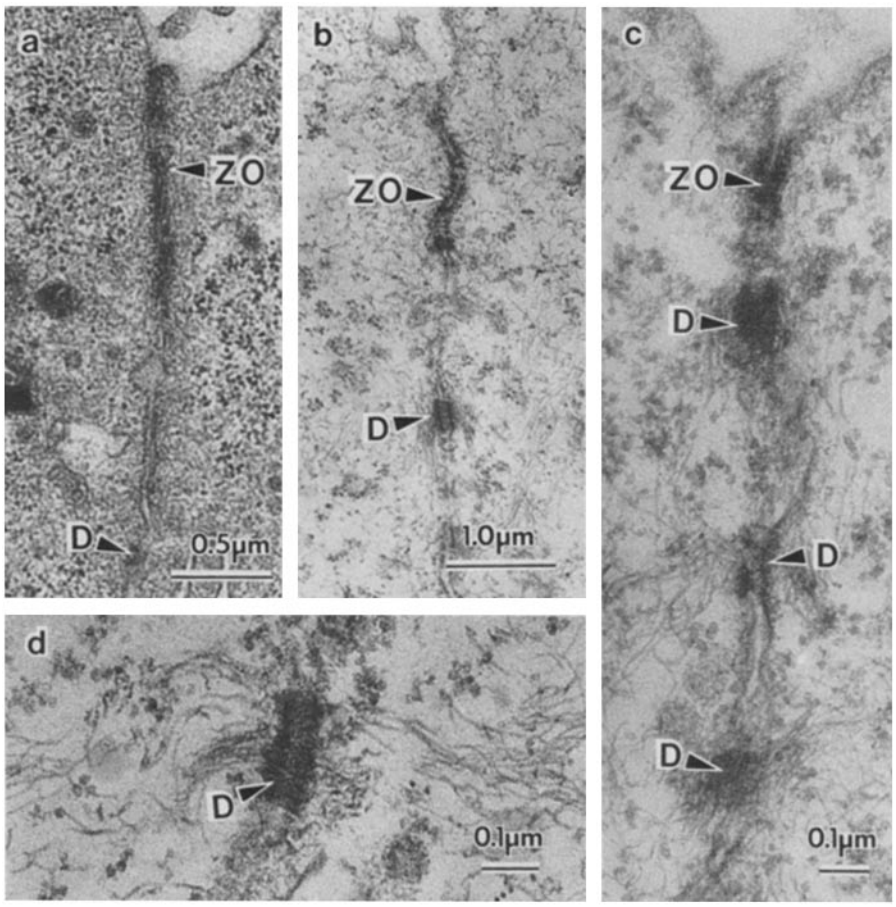


FIGURE 2 Embedded thin sections of intact and triton X-100–extracted MDCK cells. Cells were prepared and sectioned as described in Materials and Methods. The intercellular junction between two whole cells (*a*) is compared with the residual junction remaining after extraction with Triton X-100 (*b*). Zonula occludens (*ZO*) and desmosome (*D*) structures are apparent in characteristic localization after extraction. Higher magnifications of desmosomal structures after Triton X-100 extraction (*c* and *d*) reveal the retention of tonofilament (cytokeratin) associations. Note that few fibers are visible in these sections as compared to the whole mounts of identical preparations shown in Fig. 3. (*a*) × 26,000. (*b*) × 15,000. (*c*) × 55,000. (*d*) × 63,000.

## *Filament Organization in Epithelial Skeletal Frameworks*

The embedded thin sections of MDCK skeletal frameworks (Fig. 2) provide an incomplete representation of the complexity of organization inherent in these structures. When viewed in extracted, unembedded epithelial whole mounts (Fig. 3, *a* and *b*), the MDCK cytoskeleton is seen as a dense array of filaments forming a network continuous from the nuclear surface to the polygonally-ordered intercellular junctions.

It is worth emphasizing that the detergent extracted whole mounts in Fig. 3, *a* and *b*, are prepared in essentially the same way as in Fig. 2, *b–d*. Thus, the apparent difference between sections and whole mounts lies not in the preparation per se, but in the high contrast afforded by protein fibers when viewed in vacuum and their disappearance when surrounded by the hard, dense embedding plastic.

The polygonal cell boundaries (Fig. 1*c*) are seen clearly in transmission electron micrographs of skeletal frameworks prepared as whole mounts (Fig. 3, *a* and *b*). A higher magnification of the cytoskeletal networks in MDCK colonies (Fig. 3*b*) shows the dense networks of filaments with frequent fiber junctions. The cytoplasmic networks give the impression of being similarly ordered throughout the entire epithelium (Fig. 3*a*); i.e., filaments appear similarly ordered on opposite sides of cell borders, a feature that may be characteristic of tissue-forming cells. This qualitative impression is reinforced by comparing epithelial cytoskeletal networks to the skeletal frameworks of confluent, but autonomous cells that do not form tissue. The internal structures of fibroblasts, for example, appear to be quite independent in adjacent cells even in confluent monolayers (Fig. 3*c*). The filament networks in these fibroblasts are oriented with little regularity, display no intercellular junctional complexes and show no apparent continuity when cell boundaries establish contact at confluence. The epithelial MDCK cells, in sharp contrast, never grow as single cells and retain well-organized intercellular filament patterns mediated by intercellular junctions (Fig. 3, *a* and *b*).

## *NM-IF Scaffold*

The epithelial skeletal framework, obtained by extraction with Triton X-100, is further fractionated in situ to obtain the NM-IF substructure using a method previously described (10) for autonomous, single cells. An initial extraction using the CSK buffer with 0.25 M ammonium sulfate releases 23% of the total cellular protein in a fraction corresponding to the salt-labile "cytoskeleton" fraction. Chromatin, nuclear RNA, and chromatin-associated proteins are next removed by digesting with DNase I and RNase A, followed by a second elution with ammonium sulfate. This digestion-elution releases an additional 7% of the total cellular protein in a fraction termed the "chromatin"; i.e., those proteins whose association with the nucleus depends on the integrity of DNA and RNA. The NM-IF structural network remains, and consists of 5% of the total cellular protein. We suggest that this salt-resistant substructure, composed in large part of metabolically stable filaments, may serve as a scaffold for the cytoskeletal framework. The complete fractionation protocol is summarized in Fig. 4.

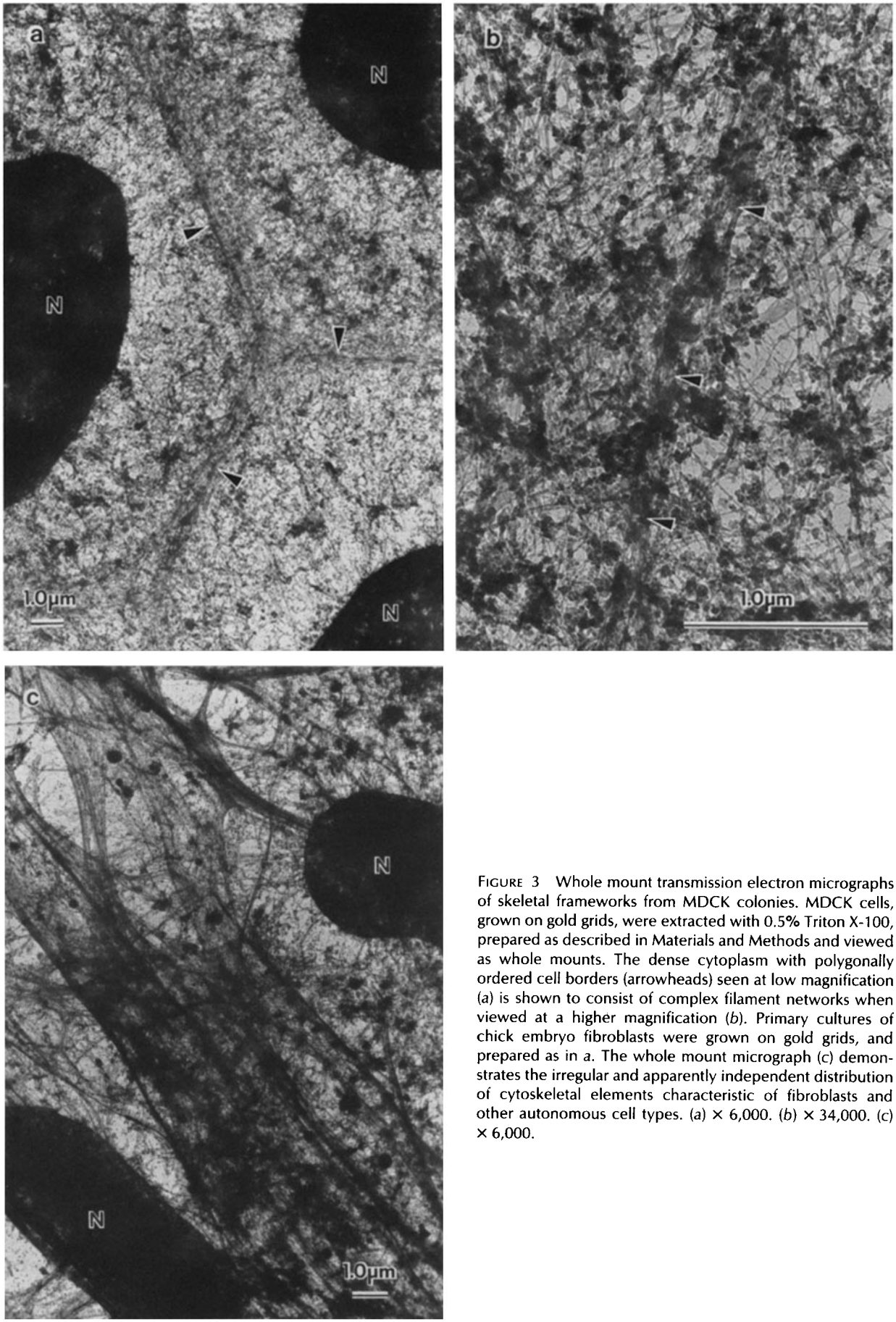


FIGURE 3 Whole mount transmission electron micrographs of skeletal frameworks from MDCK colonies. MDCK cells, grown on gold grids, were extracted with 0.5% Triton X-100, prepared as described in Materials and Methods and viewed as whole mounts. The dense cytoplasm with polygonally ordered cell borders (arrowheads) seen at low magnification (*a*) is shown to consist of complex filament networks when viewed at a higher magnification (*b*). Primary cultures of chick embryo fibroblasts were grown on gold grids, and prepared as in *a*. The whole mount micrograph (*c*) demonstrates the irregular and apparently independent distribution of cytoskeletal elements characteristic of fibroblasts and other autonomous cell types. (*a*) × 6,000. (*b*) × 34,000. (*c*) × 6,000.

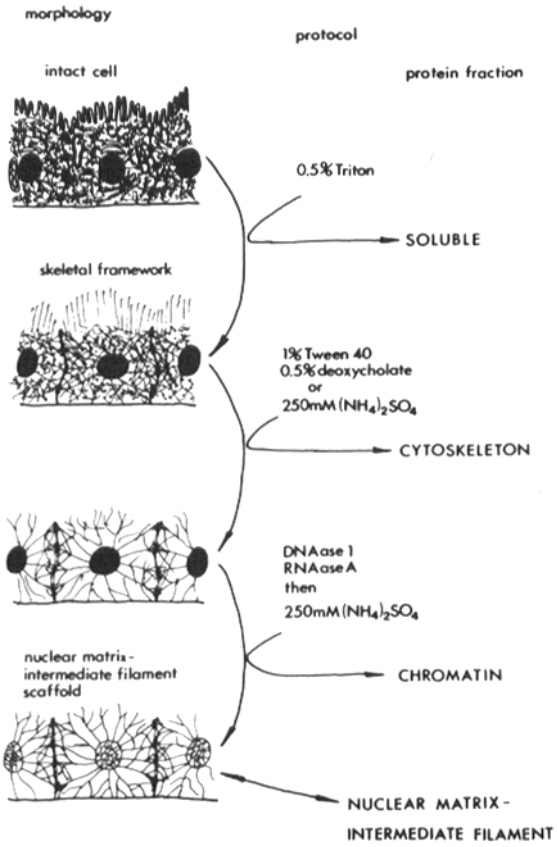


FIGURE 4 Summary of the fractionation protocol. This cartoon depicts the relationship between the morphological fractionation and the protein populations obtained after each fractionation step. The Triton X-100-soluble proteins constitute 65% of the total cell protein. The cytoskeleton, chromatin NM-IF fractions represent 23%, 7%, and 5% of the total cell protein, respectively. All of the cellular constituents are recovered in this fractionation.

## Protein Composition of Fractions

The proteins obtained in the cytoskeleton, chromatin, and NM-IF fractions, together with the soluble protein from the initial Triton X-100 extract, represent four distinct protein subsets of the cell as is shown in the two-dimensional gel electropherograms in Fig. 5. The soluble fraction represents the majority of cellular proteins and reveals a complex, dense pattern of major proteins in two-dimensional gel analysis. While many proteins appear to be unique to this fraction, the density of protein spots on this gel precludes more precise analysis of overlap between proteins in the soluble and other fractions.

The protein composition of the cytoskeleton, chromatin, and NM-IF fractions (Fig. 5) is complex, though much less so than the soluble fraction. In addition, each of these fractions has a characteristic protein pattern whose major proteins are found predominately in only one of the three fractions. Some of the proteins characteristic of each fraction are identified by arrows (Fig. 5). Careful examination shows very few proteins in more than one fraction. Thus the sequential extraction technique produces subfractions that represent biochemically distinct populations of cellular proteins, as well as morphologically distinct structures (see below).

## Immunofluorescent Localization of Proteins in the NM-IF Scaffold

Some assurance that the successive extractions, including the relatively harsh high-salt elutions, neither create new structures nor seriously distort preexisting ones, is afforded by the experiment whose results are shown in Fig. 6. The immunofluorescent patterns of four antigens, specific for the NM-IF fraction and visualized in intact cells after fixation in cold methanol, are compared to the patterns of these antigens in the NM-IF structure after successive extractions (procedures outlined in Fig. 4).

Fig. 6 *a* shows an immunofluorescence stain using a serum antibody derived to human callus keratin, which reacts with the cytokeratins (37, 38), first in the alcohol fixed intact cells (Fig. 6 *a*) and in the extracted NM-IF scaffold (Fig. 6 *b*). The pattern shows the cytokeratins to be concentrated near the cell borders although many filaments extend to the cell interiors. The similarity of the patterns in the intact and extracted cells indicates that the extraction procedure does not grossly modify the pre-existing filament distribution. The micrographs in Fig. 6, *c* and *d*, compare the distribution of vimentin, using an antiserum derived to the 58,000-mol-wt protein (39), in the intact (Fig. 6 *c*) and extracted (Fig. 6 *d*) epithelium. As is true of cultured epithelial cells in general, there is considerable vimentin synthesis that is not usually observed in epithelial cells in vivo (40–43). The vimentin distribution is also unchanged during extraction. Notable is the marked regional localization of the two types of intermediate filaments, with vimentin occupying the perinuclear region and the cytokeratins concentrated towards the cell periphery.

Fig. 6 *e* shows staining of the intact nucleus by a monoclonal antibody to an, as yet, uncharacterized 52,000-mol-wt nuclear surface antigen. The staining pattern is a diffuse nuclear fluorescence with superimposed bright patches. Both the location and shape of the staining pattern of the nuclear lamina (Fig. 6 *f*) remains unchanged by the extraction which removes chromatin as well as the cytoskeletal elements.

A serum antibody to desmosomal core proteins (44) strongly stains the cell borders where the intercellular junctions would be expected. The fluorescence pattern is interrupted, and, in some regions, punctate, suggesting that principally desmosomes (maculae adherens) are stained (Fig. 6, *g* and *h*). Again, there is little difference in the patterns at the cell borders between the fixed, intact cells (Fig. 6 *g*) and the NM-IF scaffold (Fig. 6 *h*). In this case, however, the antibody lightly stains the nucleus in the intact cells. This antigen is removed by the extraction, leaving only the fluorescence at the border. The significance of this nuclear staining is unknown and will be discussed below.

## Distribution of Proteins Observed in the NM-IF Core among Other Fractions

An immunoblot analysis of the reactivity of the four antibodies in Fig. 6 with the electrophoretically separated proteins of the individual cell fractions is shown in Fig. 7. This serves to establish the specificity of the antibodies and demonstrate the partition of these specific proteins among the four cellular fractions. Equal amounts of protein from the soluble, cytoskeleton, chromatin, and NM-IF fractions were separated by PAGE. The proteins were transferred to nitrocellulose strips that were then incubated with the four antibodies previously

used for immunofluorescence staining (Fig. 6). Bands were visualized using the horseradish peroxidase–second antibody technique described in Materials and Methods.

The immunoblot patten for vimentin is particularly simple as essentially all of this 58,000-mol-wt protein is found in the NM-IF scaffold fraction, with only a trace appearing in the cytoskeleton (Fig. 7). Some lightly staining bands of lower molecular weight are seen in the NM-IF fraction. These may be due to a small amount of proteolysis or some cross-reactivity with other matrix proteins by this antibody preparation. The principal cytokeratins are also found exclusively in the NM-IF scaffold fraction. The bands correspond to proteins of 40,000, 42,000, 52,000, 56,000, and 58,000 mol wt (Fig. 7). There are very faint bands corresponding to the 58,000-mol-wt cytokeratin in the soluble cytoskeleton and chromatin fractions. These proteins represent <1% of the total cytokeratin in the cell. The significance of this population of cytokeratin is not obvious, it could conceivably represent a pool of soluble precursors as reported for vimentin (45).

The protein corresponding to the nuclear antigen stained by the monoclonal antibody is ~52,000 mol wt and is found exclusively in the NM-IF scaffold (Fig. 7). It is too low in molecular weight to be a nuclear lamin (46, 47). A very lightly staining band at ~42,000 mol wt is seen in the skeletal framework and NM-IF fraction; its significance is unknown.

The immunoblot pattern of the serum antibody to desmosomal core protein is complicated. Three principal bands at 240,000, 210,000, and 150,000 mol wt corresponding to the desmosome plaque proteins and glycoproteins described by Cohen et al. (44) are found only in the NM-IF scaffold (Fig. 7). A 56,000-mol-wt protein, probably a cytokeratin, also reacts with this serum antibody, but only in the NM-IF fraction. Several other bands are stained in the other fractions and their relation to desmosome core structure, if any, is unknown. Some of these detergent or salt extractable proteins may correspond to the proteins responsible for nuclear fluorescence in the intact cells in Fig. 6*d*.

## *Whole Mount Electron Microscopy of the NM-IF Scaffold*

The NM-IF scaffold preparation, consisting of only 5% of the total cellular protein, affords striking images when exam-

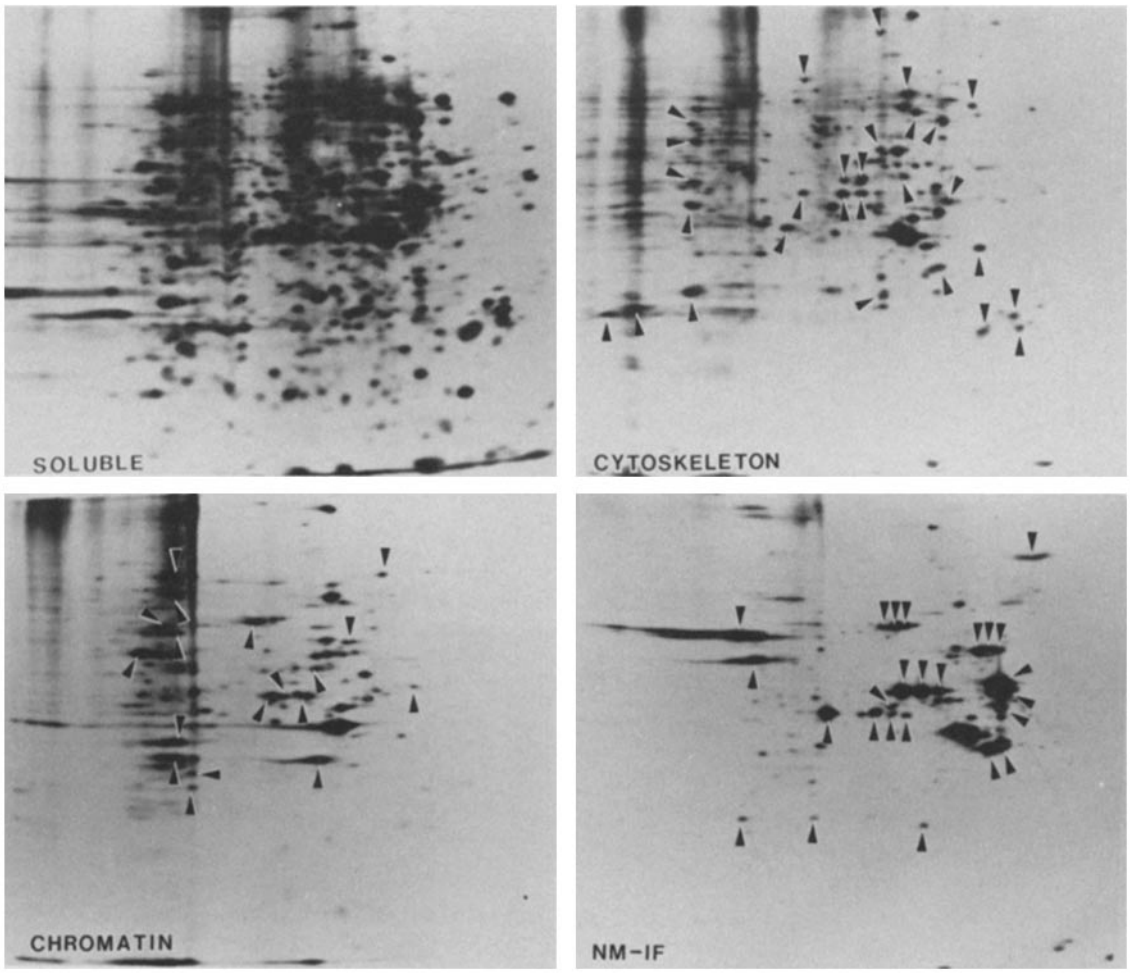


FIGURE 5 Two-dimensional gel profiles of proteins obtained after fractionation of MDCK colonies. Fractionation and two-dimensional gel electrophoresis were carried out as described in Materials and Methods. The first dimension ranges from pH 10 to pH 3 (left to right). The patterns of the cytoskeleton, chromatin, and *NM-IF* fractions are individually characteristic with little overlap of protein from one fraction to another. Major proteins that are found predominately in only one of these fractions are indicated by arrowheads.

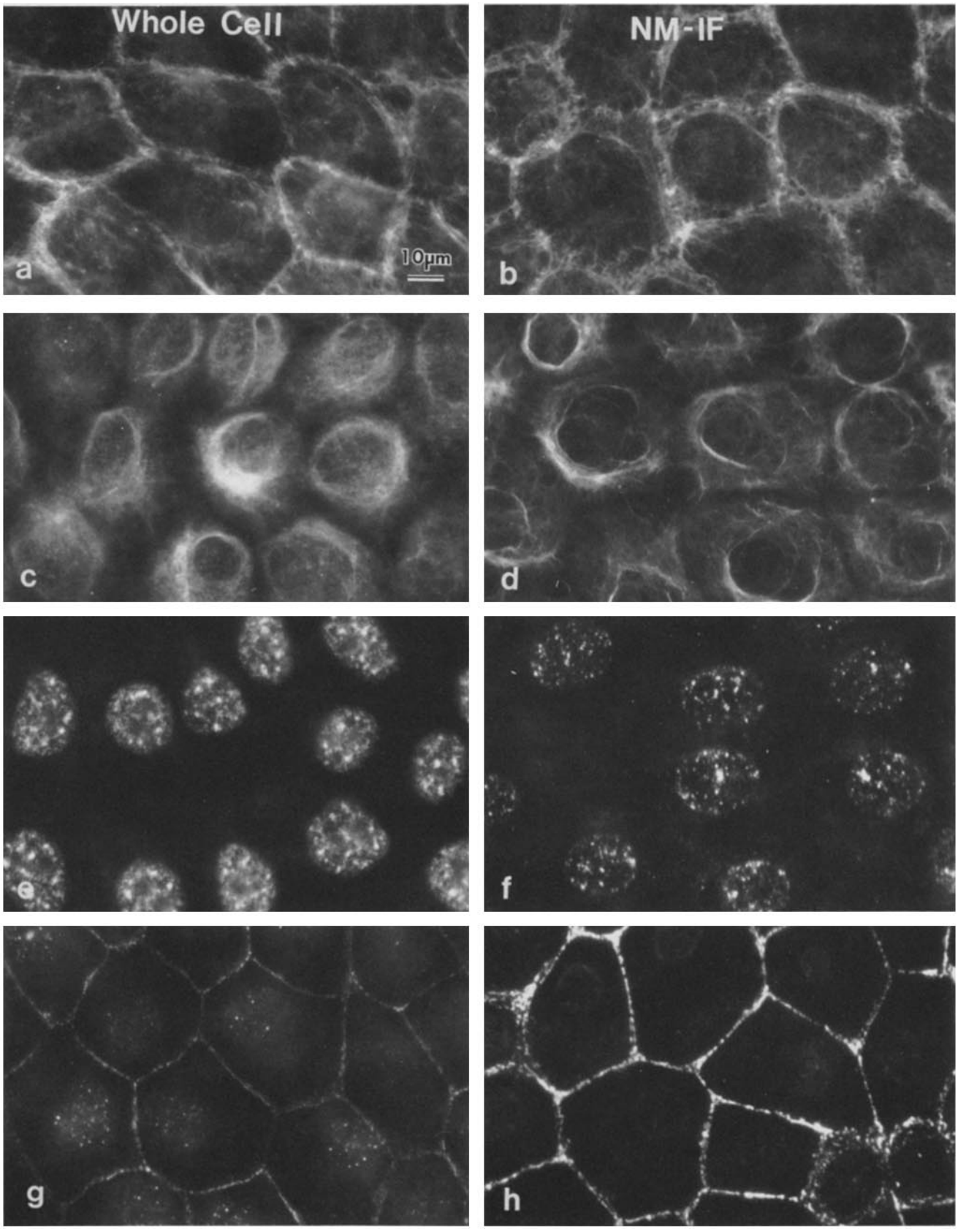
Whole Cell
NM-IF
10μm
a
b
c
d
e
f
g
h

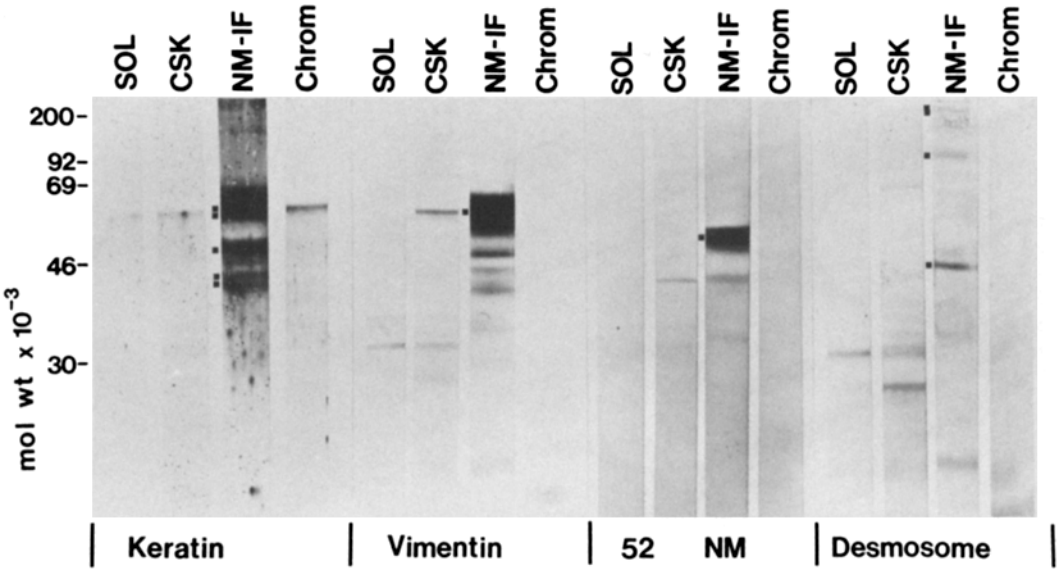


FIGURE 7 Identification of keratin, vimentin, a 52,000-mol-wt nuclear matrix protein (*52 NM*) and the desmosomal core proteins in individual MDCK fractions. Aliquots representing equivalent protein concentrations from the soluble (*SOL*), cytoskeleton (*CSK*), *NM-IF*, and chromatin (*Chrom*) fractions were separate on 10% polyacrylamide gels and transferred to nitrocellulose as described in Materials and Methods. Bound antibodies were labeled using a second antibody conjugated to horseradish peroxidase as described. The keratins, vimentin and the 52,000-mol-wt nuclear matrix proteins are found predominantly in the NM-IF fraction in these immunoblots where the major protein bands are saturated. There is minimal staining of these bands in fractions other than the NM-IF core. Keratins with molecular weights of 58,000, 56,000, 52,000, 42,000, and 40,000 are indicated as in the 58,000-mol-wt vimentin band and the 52,000-mol-wt nuclear matrix protein. The distribution of desmosomal core proteins is more complex, with the bands at 230,000, 205,000, and 150,000 mol wt found only in the NM-IF fraction. A 50,000-mol-wt band which reacts with the desmosome core antiserum is also uniquely present in the NM-IF core (see text).

ined by whole mount transmission electron microscopy. Apical views of the NM-IF scaffold derived from an MDCK epithelial sheet are shown in Fig. 8. The filament network is much simpler in composition and overall organization than the skeletal framework. However, after removal of phospholipid, nucleic acids, and 95% of the total cellular protein, the remaining structure still clearly retains the organization characteristic of an epithelium. The polygonal outline of the epithelial cells is still identifiable from the remnant cell boundary stuctures. Included in these boundaries are dense plaques that serve as termini for bundles of filaments. From their location and association with the intermediate filaments, these dense plaques are most probably the remnant desmosomal structures and are so identified by immunoelectron microscopy (Fig. 8*d*). A web of filaments, most of ~10 nm in diameter, many originating at the nuclear surface, extend throughout most of the cytoplasmic space. This is consistent with the observation of numerous interconnected filaments characteristic of the organization of cytokeratins in intact epithelia (see Discussion). In the NM-IF network, numerous filaments appear to originate on the surface of the nuclear matrix (Fig. 8, *a* and *b*) and many terminate at the dense plaques or desmosomes of the remnant junctional complexes (Fig. 8*c*). Some of these fibers form direct connections between the desmosomes and the nuclear matrix.

The identification of the dense plaques at the remnant cell boundaries as desmosomes was made on the basis of their location and their apparent role as termini for many intermediate filaments. A direct demonstration of the identity of these plaques in whole mount transmission electron microscopy is afforded by reacting the structure with antidesmosome protein antibody and a second antibody conjugated to gold

FIGURE 6 Immunofluorescent localization of keratins, vimentin, a 52,000-mol-wt nuclear matrix protein and desmosomal proteins in whole MDCK epithelial monolayers and the NM-IF scaffold. Whole MDCK colonies were fixed in methanol at −20°C and postfixed in formaldehyde as described in Materials and Methods. NM-IF core structures were prepared from identical colonies and fixed as described in the Materials and Methods section. The antibody-second antibody reactions were carried out as described in Materials and Methods. In each case, the appropriate second antibody was conjugated to tetramethylrhodamine isothiocyanate. Keratins were localized using a serum antibody derived against total urea-insoluble, urea/mercaptoethanol-soluble material from human callus (see Wu and Rheinwald and Wu et al. [37, 38]) in both whole (*a*) and NM-IF fractionated (*b*) MDCK colonies. Vimentin localization in whole (c) and NM-IF fractionated colonies (*d*) was analysed using a serum antibody derived to 58,000-mol-wt vimentin (see Hynes and Destre [39]). A monoclonal antibody reacts with a 52,000-mol-wt protein from the nuclear matrix was prepared as described. The localization of 52,000-mol-wt protein in the nucleus of whole (e) and NM-IF fractionated MDCK cells (*f*) is essentially unchanged by the fractionation protocol. The desmosomal core proteins were localized using a serum antibody to isolated desmosomes (see Gorbsky and Steinberg [19]). The whole cells (*g*) show punctate fluorescent staining at the intercellular junctions which is entirely retained in the NM-IF fractionated colonies (*h*). The nuclear fluorescence observed in the whole cells is removed during the fractionation and may correspond to a unique subset of proteins that react with this antibody (see Fig. 7). × 650.

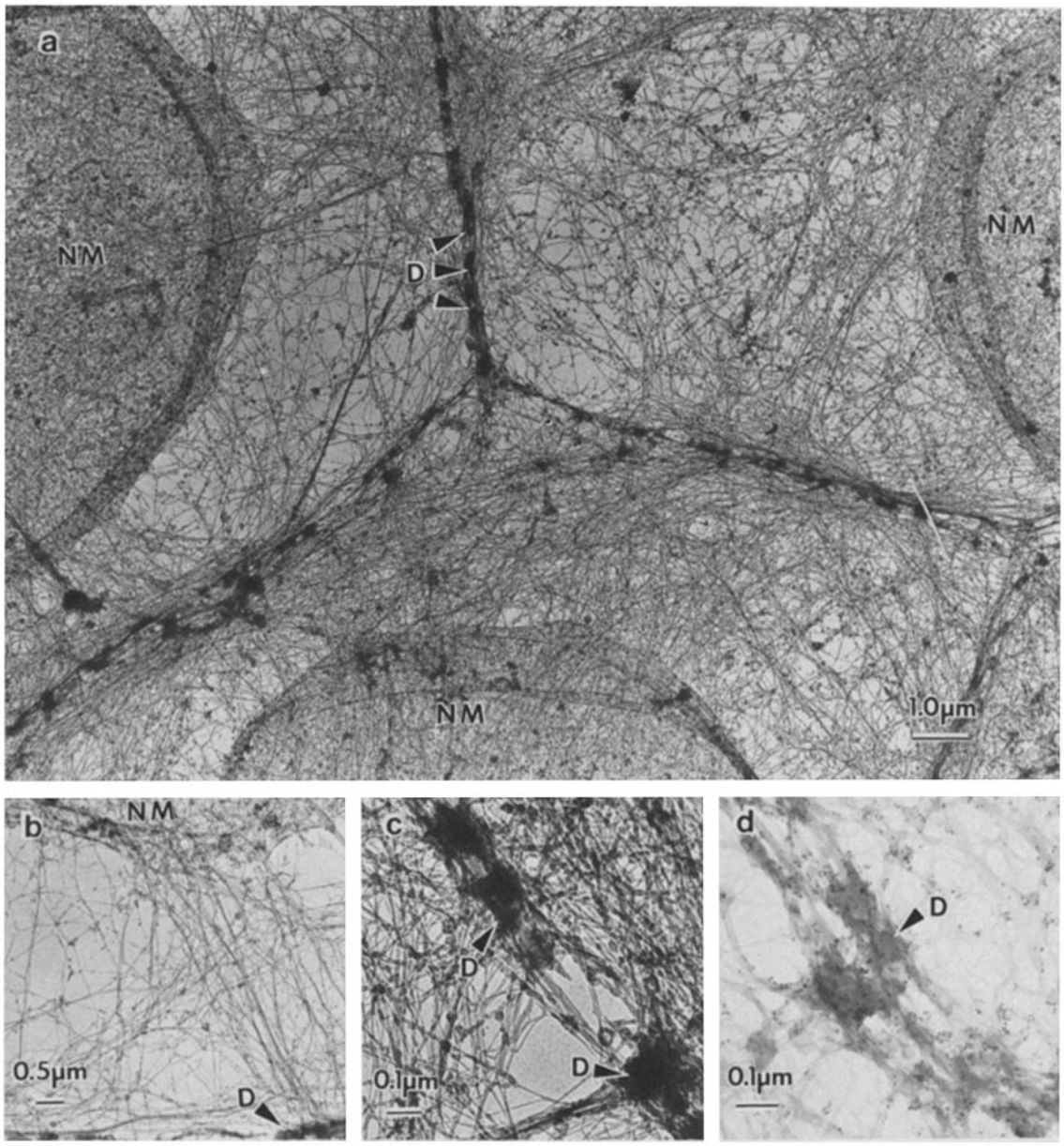


FIGURE 8 NM-IF scaffold of an MDCK epithelium. After further fractionation of the skeletal framework (shown in Fig. 3) as described in Materials and Methods this structure, representing only 5% of the total cell protein, is viewed in whole mount transmission microscopy. The chromatin-depleted nuclear matrices (*NM*) (*a*) are apparent in association with cytoplasmic filaments largely consisting of cytokeratins (see Fig. 6), which often terminate in residual desmosome structures (*D*). High magnifications of this fraction detail the nuclear matrix (*b*) and desmosomal complex (*c*) structures. NM-IF core structures were fixed and antibody reactions were carried out with desmosomal antiserum followed by a second antibody conjugated to gold beads as described in the Materials and Methods. Greater than 75% of the gold bead staining from this antibody is observed in the dense structures (*d*) which are tentatively identified as residual desmosomal cores (arrowheads). (*a*) × 6,000. (*b*) × 8,000. (*c*) × 50,000. (*d*) × 60,000.

beads. Clear images of the gold bead staining are afforded by the whole mounts (Fig. 8*d*).

## DISCUSSION

### *Fractionation Protocol*

In this study, epithelial cell colonies were sequentially fractionated producing first the Triton X-100–resistant skeletal framework, and then the nuclease and salt-resistant NM-IF scaffold. These structures represent morphological endpoints in a fractionation scheme that divides the epithelium into four biochemically distinct protein populations. The retention of a specific subset of cellular proteins in each of the four fractions allows for a reproducible analysis of biochemical events in which skeletal elements are involved. Because all of the cellular proteins are retained during the course of fractionation, quantitative analyses of rates of synthesis, phosphorylation and assembly of structural elements are possible.

### *NM-IF Scaffold*

Of the four protein fractions that were obtained in the procedure described in this report, the NM-IF core is of particular relevance to the differentiated epithelial state. Both cytokeratins and desmosomal core proteins are characteristic of epithelial cells. Both classes of proteins are quantitatively retained in the NM-IF scaffold (Fig. 7) but not observed in the NM-IF fraction from fibroblasts (see reference 10). Al-

though the resistance to extraction by detergent and salt of both the cytokeratins and desmosome proteins is well-established (18, 19, 44, 48), the participation of these elements in an independent and ordered structure involving the nuclear matrix is observed here for the first time.

The NM-IF scaffold is a continuous structure that extends throughout the entire epithelial sheet and retains the spatial disposition of nuclei and junctional complexes after the removal of phospholipid, nucleic acids, and 95% of the cellular proteins. The morphological distribution and association of desmosomes, cytokeratin filaments (or tonofilaments), and the nuclear matrix observed in the NM-IF scaffold are in agreement with a number of earlier studies of epithelial cells and tissues.

The nuclear matrix is a fibrillar protein complex (10, 49–51), which retains nuclear pore complexes (52), is associated with heterogeneous nuclear RNA (53–55) and replicating DNA (56–59). The role of the nuclear matrix in nuclear function is not clearly understood, but the stable association between the nuclear matrix and intermediate filaments (Fig. 8) suggest that a spatial ordering of the nucleus might be mediated by the NM-IF in vivo. The association between intermediate filaments and intact nuclei has been frequently reported (10, 21, 22, 60, 61).

The extensive networks of tonofilaments in epithelial cells is a longstanding observation (14, 62), which has been demonstrated using immunofluorescent microscopy in both intact epithelia from whole tissue (42, 63–66) and from cultured epithelial cells (15–17, 20, 67). In the present study, this network of filaments is quantitatively isolated and shown to retain its complex structure with considerable fidelity (Fig. 6).

At the residual cellular junctions of the NM-IF core, the desmosomal proteins are observed in a linear, punctate pattern. This pattern corresponds to the polygonal cell boundaries observed in intact epithelia (Fig. 6). The desmosomal structures also serve as nexi for numerous cytokeratin filaments (14, 18, 19, 44, 48, 62; and Fig. 8). Thus, these remnant junctional complexes retain the intercellular continuity of the epithelium in isolation. These data are consistent with the model of Hull and Staehelin (62) who suggest that a continuous mechanical coupling is provided between cytoskeletal networks of adjacent epithelial cells by tonofilament interactions of desmosomes. However, the model of epithelial organization suggested by the NM-IF scaffold differs from that proposed above (62) in that the nuclear matrix is intimately involved in the scaffold organization.

We are grateful to Gabriella Krochmalnic and David Cummings for assistance in electron microscopy. We wish to thank Patricia Turner for preparing the manuscript. We also wish to thank Drs. J. Rheinwald, M. Steinberg, and R. Hynes for generously providing antikeratin, antidesmosomal and antivimentin antibodies.

This work was supported by grant funds from the National Science Foundation and National Institutes of Health to Sheldon Penman.

*Received for publication 29 August 1983, and in revised form 1 February 1984.*

## REFERENCES

1. Lenk, R., L. Ransom, Y. Kaufmann, and S. Penman. 1977. A cytoskeletal structure with associated polyribosomes obtained from HeLa cells. *Cell.* 10:67–78.
2. Lenk, R., and S. Penman. 1979. The cytoskeletal framework and poliovirus metabolism. *Cell.* 16:289–301.
3. Small, J. V., and J. E. Celis. 1978. Direct visualization of the 10nm (100A)-filament network in whole and enucleated cultured cells. *J. Cell Sci.* 31:393–409.
4. Webster, R. S., D. Henderson, M. Osborn, and K. Weber. 1978. Three-dimensional electron microscopical visualization of the cytoskeleton of animal cells: immunoferritin identification of actin-and-tubulin-containing structures. *Proc. Natl. Acad. Sci. USA.* 75:5511–5515.
5. Ben-Zeev, A., A. Duerr, F. Solomon, and S. Penman. 1979. The outer boundary of the cytoskeleton: a lamina derived from plasma membrane proteins. *Cell.* 17:859–865.
6. Fulton, A. B., K. M. Wan, and S. Penman. 1980. The spatial distribution of polyribosomes in 3T3 cells and the associated assembly of proteins into the skeletal framework. *Cell.* 20:849–857.
7. Cervera, M., G. Dreyfuss, and S. Penman. 1981. Messenger RNA is translated when associated with the cytoskeletal framework in normal and VSV-infected HeLa cells. *Cell.* 23:113–120.
8. Schliwa, M., and J. Van Blerkom. 1981. Structural interaction of cytoskeletal components. *J. Cell Biol.* 90:222–235.
9. Schliwa, M. 1982. Action of cytochalasin D on cytoskeletal networks. *J. Cell Biol.* 92:79–91.
10. Capco, D. G., K. M. Wan, and S. Penman. 1982. The nuclear matrix: three-dimensional architecture and protein composition. *Cell.* 29:847–858.
11. Madin, S. H., and N. B. Darby. 1975. American Type Culture Collection Catalogue of Strains II. First Edition. American Type Culture Collection, Rockville, MD. 47.
12. McRoberts, J. A., M. Taub, and M. H. Saier. 1981. The Madin Darby canine kidney (MDCK) cell line. *In* Fuctionally Differentiated Cell Lines. G. Sato, ed. Alan R. Liss, New York. 117–139.
13. Rodriquez-Boulan, E., and D. D. Sabatini. 1978. Asymmetric budding of viruses in epithelial monolayers: a model system for study of epithelial polarity. *Proc. Natl. Acad. Sci. USA.* 75:5071–5075.
14. Faraguhar, M. G., and G. E. Palade. 1963. Junctional complexes in various epithelia. *J. Cell Biol.* 17:375–412.
15. Franke, W. W., K. Weber, M. Osborn, E. Schmid, and C. Freudenstein. 1978. Antibody to prekeratin: decoration of tonofilament-like arrays in various cells of epithelial character. *Exp. Cell Res.* 116:429–445.
16. Sun, T. T., and H. Green. 1978. Immunofluorescent staining of keratin fibers in cultured cells. *Cell.* 14:469–476.
17. Franke, W. W., E. Schmid, K. Weber, and M. Osborn. 1979. HeLa cells contain intermediate-sized filaments of the prekeratin type. *Exp. Cell Res.* 118:95–109.
18. Franke, W. W., S. Winter, C. Grand, E. Schmid, D. L. Schiller, and E. Jarasch. 1981. Isolation and characterization of desmosome-associated tonofilaments from rat intestinal brush border. *J. Cell Biol.* 90:116–127.
19. Gorbsky, G., and M. S. Steinberg. 1981. Isolation of the intercellular glycoproteins of desmosomes. *J. Cell Biol.* 90:243–248.
20. Schmid, E., D. L. Schiller, C. Grund, J. Stadler, and W. W. Franke. 1983. Tissue type-specific expression of intermediate filament proteins in a cultured epithelial cell line from boving mammary gland. *J. Cell Biol.* 96:37–50.
21. Lehto, V. L., I. Virtanen, and P. Kurki. 1978. Intermediate filaments anchor the nuclei in nuclear monolayers of cultured human fibroblasts. *Nature (Lond.).* 272:175–177.
22. Staufenbiel, M., and W. Deppert. 1982. Intermediate filament systems are collapsed onto the nuclear surface after isolation of nuclei from tissue culture cells. *Exp. Cell Res.* 138:207–214.
23. Galfre, G., S. C. Howe, C. M. Milstein, G. W. Butcher, and J. C. Howard. 1977. Antibodies to the major histocompatibility antigens produced by hybrid cell lines. *Nature (Lond.).* 266:550–552.
24. Laemmli, U. D. 1970. Cleavage of structural proteins during the assembly of the head of bactereograph T4. *Nature (Lond.).* 227:680–685.
25. Towbin, H., T. Staehelin, and J. Gordon. 1979. Electrophoretic transfer of proteins from polyacrylamide gels to nitrocellulose sheets. Procedures and some applications. *Proc. Natl. Acad. Sci. USA.* 76:4350–4354.
26. Hawkes, R., E. Niday, and J. Gordon. 1982. A dot-immunobinding assay for monoclonal and other antibodies. *Anal. Biochem.* 119:142–147.
27. O'Farrell, P. H. 1975. High-resolution two-dimensional electrophoresis of proteins. *J. Biol. Chem.* 250:4007–4021.
28. Louvard, D. 1980. Apical membrane aminopeptidase appears at site of cell-cell contact in cultured kidney epithelial cells. *Proc. Natl. Acad. Sci. USA.* 77:4132–4136.
29. Richardson, J. C. W., and N. L. Simmons. 1979. Demonstration of protein asymmetries in the plasma membrane of cultured renal (MDCK) epithelial cells by lactoperoxidase-mediated iodination. *Fed. Eur. Bioch. FEBS Lett.* 105:201–204.
30. Hoi Sang, U., M. H. Saier, and M. H. Ellisman. 1979. Tight junction formation is closely linked to the polar redistribution of intramembranous particles in aggregating MDCK epithelia. *Exp. Cell Res.* 122:384–391.
31. Hoi Sang, U., M. H. Saier, and M. H. Ellisman. 1980. Tight junction formation in the establishment of intramembranous particle polarity in aggregating MDCK cells. *Exp. Cell Res.* 128:233–235.
32. Lamb, J. F., P. Ogden, and M. L. Simmons. 1981. Autoradiographic localization of [$^3$H]ouabain bound to cultured epithelial cell monolayers of MDCK cells. *Biochem. Biophys. Acta.* 644:333–340.
33. Kessel, R. G., and R. H. Kardon. 1979. Tissues and Organs: A Test-Atlas of Scanning Electron Microscopy. W. H. Freeman and Co., San Francisco. 239.
34. Aaronson, P. R., and G. Blobel. 1974. On the attachment of the nuclear pore complex. *J. Cell Biol.* 62:746–754.
35. Mooseker, M. S. 1976. Microvillar contraction in Triton-treated brush borders isolated from intestinal epithelium. *J. Cell Biol.* 71:417–432.
36. Fulton, A. B., J. Prives, S. R. Farmer, and S. Penman. 1981. Developmental reorganization of the skeletal framework and its surface lamina in fusing muscle cells. *J. Cell Biol.* 91:103–112.
37. Wu, Y.-J., and J. G. Rheinwald. 1981. A new small (40Kd) keratin filament protein made by some cultures human squomous cell carcinomas. *Cell.* 25:627–635.
38. Wu, Y.-J., L. M. Parker, N. E. Binder, M. A. Beekett, J. H. Sinard, C. T. Griffiths, and J. G. Rheinwald. 1982. The mesothelial keratins: a new family of cytoskeletal proteins identified in cultured mesothelial cells and nonkeratinizing epithelia. *Cell.* 31:693–703.
39. Hynes, R. O., and A. T. Destree. 1978. 10nm filaments in normal and transformed cells. *Cell.* 13:151–163.
40. Franke, W. W., E. Schmid, S. Winter, J. Osborn, and K. Weber. 1979. Widespread occurence of intermediate-sized filaments of the vimentin-type in cultured cells from diverse vertebrates. *Exp. Cell Res.* 123:25–46.
41. Franke, W. W., D. Mayer, E. Schmid, H. Denk, and E. Borenfreund. 1981. Differences of expression of cytoskeletal proteins in cultured rat hepatocytes and hepatoma cells. *Exp. Cell Res.* 134:345–365.
42. Summerhayes, I. C., Y.-S. Cheng, T.-T. Sun, and L. B. Chen. 1981. Expression of keratin and vimentin intermediate filaments in rabbit bladder epithelial cells at different stages of benzo(a)pyrene-induced neoplastic progression. *J. Cell Biol.* 90:63–69.

43. Virtanen, I., V.-P. Lehto, E. Lehtonen, T. Vartio, S. Stenman, P. Kurki, O. Wagner, J. V. Small, D. Dahl, and R. A. Badley. 1981. Expression of intermediate filaments in cultured cells. *J. Cell Sci.* 50:45–63.
44. Cohen, S. M., G. Gorbsky, and M. S. Steinberg. 1983. Immunochemical characterization of related families of glycoproteins in desmosomes. *J. Biol. Chem.* 258:2621–2627.
45. Blikstad, I., and E. Lazarides. 1983. Vimentin filaments are assembled from a soluble precursor in avian erythroid cells. *J. Cell Biol.* 96:1803–1808.
46. Gerace, L., A Blum, and G. Blobel. 1978. Immunocytochemical localization of the major polypeptides of the nuclear pore complex-lamina fraction. *J. Cell Biol.* 79:546–566.
47. Fisher, P. A., M. Berrios, and G. Blobel. 1982. Isolation and characterization of a proteinaceous subnuclear fraction composed of nuclear matrix, peripheral lamina, and nuclear pore complexes from embryos of drosophila melanogastes. *J. Cell Biol.* 92:674–686.
48. Drochmans, P., C. Freudenstein, J. C. Wanson, L. Laurent, T. W. Keenan, J. Stadler, R. Leloup, and W. W. Franke. 1979. Structure and biochemical composition of desmosomes and tonofilaments isolated from calf muzzle epidermis. *J. Cell Biol.* 79:427–443.
49. Berezney, R., and D. S. Coffey. 1974. Identification of a nuclear protein matrix. *Biochem. Biophys. Res. Commun.* 60:1410–1417.
50. Commings, D. E., and T. A. Okada. 1976. Nuclear proteins III. The fibrillar nature of the nuclear matrix. *Exp. Cell Res.* 103:341–360.
51. Kaufmann, S. H., D. S. Coffey, and J. H. Shaper. 1981. Considerations in the isolation of rat liver nuclear matrix, nuclear envelope, and pore complex lamina. *Exp. Cell Res.* 132:105–123.
52. Aaronson, R. P., and G. Blobel. 1975. Isolation of nuclear pore complexes in association with lamina. *Proc. Natl. Acad. Sci. USA.* 72:1007–1011.
53. Herman, R., L. Weymouth, and S. Penman. 1978. Heterogeneous nuclear RNA-protein fibers in chromatin depleted nuclei. *J. Cell Biol.* 78:663–674.
54. Miller, T. E., C. Y. Huang, and O. A. Pogo. 1978. Rat liver nuclear skeleton and ribonucleoprotein complexes containing hnRNA. *J. Cell Biol.* 76:675–691.
55. Van Eekelen, C. A. G., and W. J. van Venrooij. 1981. hnRNA and its attachment to a nuclear protein matrix. *J. Cell Biol.* 88:554–563.
56. Dijkwel, P. A., L. H. F. Mullenders, and F. Wanka. 1979. Analysis of the attachment of replicating DNA to a nuclear matrix in mammalian interphase nuclei. *Nucleic Acids Res.* 6:219–230.
57. Berezney, R., and D. S. Coffey. 1975. Nuclear protein matrix: association with newly synthesized DNA. *Science (Wash. DC).* 189:291–293.
58. Pardoll, D. M., B. Vogelstein, and D. S. Coffey. 1980. A fixed wite of DNA replication in eucaryotic cells. *Cell.* 19:527–536.
59. Berezney, R., and L. A. Buchholtz. 1981. Dynamic association of replicating DNA fragments with the nuclear matrix of regenerating a liver. *Exp. Cell Res.* 132:1–13.
60. Woodcock, C. L. F. 1980. Nucleus-associated intermediate filaments from chicken erythrocytes. *J. Cell Biol.* 85:881–889.
61. Granger, B. L., and E. Lazarides. 1982. Structural associations of synemin and vimentin filaments in avian erythrocytes revealed by immunoelectron microscopy. *Cell.* 30:263–275.
62. Hull, B. E., and L. A. Staehelin. 1979. The terminal web, a reevaluation of its structure and function. *J. Cell Biol.* 81:67–82.
63. Sun, T.-T., C. Shih, and H. Green. 1979. Keratin cytoskeletons in epithelial cells of internal organs. *Proc. Natl. Acad. Sci. USA.* 76:2813–2817.
64. Tseng, S. C. G., M. J. Jarvinen, W. G. Nelson, J.-W. Huang, J. Woodcock-Mitchell, and T.-T. Sun. 1982. Correlation of specific keratins with different types of epithelial differentiation: monoclonal antibody studies. *Cell.* 30:361–372.
65. Milstone, L. M., and J. McGuire. 1981. Different polypeptides form the intermediate filaments in bovine hoof and esophageal epithelium and in aortic endothelium. *J. Cell Biol.* 88:312–316.
66. Moll, R., W. W. Franke, B. Volc-Platzer, and R. Krepler. 1982. Different keratin polypeptides in epidermis and other epithelia of human skin: a specific cytokeratin of molecular weight 46,000 in epithelia of the pilosebaceous tract and basal cell epitheliomas. *J. Cell Biol.* 95:285–295.
67. Lane, E. B., S. L. Goodman, and C. K. Trejdcsiewica. 1982. Disruption of the keratin filament network during epithelial cell division. *EMBO (Eur. Mol. Biochem. Organ.) J.* 1:1365–1372.